

Adaptive Evolutionary Programming with Neural Network for Transient Stability Constrained Optimal Power Flow

Kritsana Tangpatiphan, *Student Member, IEEE*, and Akihiko Yokoyama, *Member, IEEE*

Abstract—An adaptive evolutionary programming (AEP) with a neural network is presented to solve transient stability constrained optimal power flow (TSCOPF). The AEP adjusts its population size automatically during an optimization process to obtain the TSCOPF solution. The artificial neural network is embedded into AEP to reduce the computational load caused by transient stability constraints. The fuel cost minimization is selected as the objective function of TSCOPF. The proposed method is tested on the IEEE 30-bus system with two types of the fuel cost functions, i.e. the conventional quadratic function and the quadratic function superimposed by sine component to model the cost curve without and with valve-point loading effects respectively. The numerical examples show that AEP is more effective than conventional EP in searching the global solution, and when the neural network is incorporated into AEP, it can significantly enhance the computational speed. A study of the architecture of the neural network is also conducted and discussed.

Index Terms—Artificial neural network, evolutionary programming, power system operation, transient stability constrained optimal power flow.

I. INTRODUCTION

Optimal power flow (OPF) is one of the optimization problems in power system operation basically aiming at setting the control variables of power system to optimize a selected objective function while meeting all related static constraints simultaneously [1]. Recently, due to several blackouts caused by transient instability, dynamic constraints are added into OPF to guarantee transient stability of the power system against possible contingencies. This problem is so called transient stability constrained optimal power flow (TSCOPF) [2].

Although the conventional optimization methods, such as primal-dual Newton interior-point method [3] and linear programming (LP) [2] are applied to solve the TSCOPF problem effectively, these methods have many limitations and some drawbacks. Therefore, the modern heuristic optimization methods have recently become more and more attractive to researchers for solving the TSCOPF problem. Some of them are particle swarm optimization (PSO) [4], improved genetic algo-

rithm (GA) [5], and differential evolution (DE) [6]. Nevertheless, to apply these methods, one of the main parameters in the mentioned heuristic methods, i.e. swarm size of PSO or population size of GA and DE, is needed to be predefined. The selection of the suitable population or swarm size in order to get the good result is a difficult task and relies on the several trials and error with different parameter sets.

To avoid the problem, the adaptive evolutionary programming (AEP) is proposed as a main optimizer for TSCOPF in this paper. The population size of AEP is automatically adjusted based on the quality of the population. The population adaptation rule is based on the idea of removing or adding a particle in TRIBES PSO [7]. Moreover, the proposed neural network and time-domain simulation are incorporated in the AEP to deal with transient stability constraints. The advent of the neural network will enhance the computation speed by avoiding the unnecessary use of the time-domain simulation.

This paper is organized as follows. Section II gives a brief review of the TSCOPF problem formulation. Section III explains the proposed neural network for transient stability assessment. Section IV highlights the main components of the proposed method. Section V provides the simulation results and discussion. Finally, conclusion is given in the Section VI.

II. TSCOPF PROBLEM FORMULATION

A. Objective Function

The minimization of the total fuel cost function mathematically expressed in (1) is the TSCOPF objective function.

$$F = \sum_{i=1}^{NG} f_i(P_{Gi}) \quad (1)$$

where F is the total fuel cost; $f_i(P_{Gi})$ is the fuel cost function of the i -th generator; P_{Gi} is the active power output of the i -th generator; NG is the number of generating units.

B. Constraints

Equality and inequality constraints are defined as follows:

$$P_{Gi} - P_{Di} - V_i \sum_{j=1}^N V_j (G_{ij} \cos \theta_{ij} + B_{ij} \sin \theta_{ij}) = 0 \quad i = 1, 2, \dots, N \quad (2)$$

$$Q_{Gi} - Q_{Di} - V_i \sum_{j=1}^N V_j (G_{ij} \sin \theta_{ij} - B_{ij} \cos \theta_{ij}) = 0 \quad i = 1, 2, \dots, N \quad (3)$$

Kritsana Tangpatiphan is with the Department of Electrical Engineering, the University of Tokyo, Tokyo, 113-8656 Japan (e-mail: kritsana@syl.t.u-tokyo.ac.jp).

Akihiko Yokoyama is with the Department of Advanced Energy, the University of Tokyo, Chiba, 277-8568 Japan (e-mail: yokoyama@syl.t.u-tokyo.ac.jp).

$$P_{Gi,\min} \leq P_{Gi} \leq P_{Gi,\max} \quad i = 1, 2, \dots, NG \quad (4)$$

$$Q_{Gi,\min} \leq Q_{Gi} \leq Q_{Gi,\max} \quad i = 1, 2, \dots, NG \quad (5)$$

$$V_{i,\min} \leq V_i \leq V_{i,\max} \quad i = 1, 2, \dots, N \quad (6)$$

$$T_{i,\min} \leq T_i \leq T_{i,\max} \quad i = 1, 2, \dots, NT \quad (7)$$

$$|S_{Li}| \leq S_{Li,\max} \quad i = 1, 2, \dots, NL \quad (8)$$

$$\dot{\delta}_i = \omega_i - \omega_R \quad i = 1, 2, \dots, NG \quad (9)$$

$$2H_i \dot{\omega}_i = \omega_R (P_{mi} - P_{ei} - D_i \omega_i) \quad i = 1, 2, \dots, NG \quad (10)$$

$$|\delta_i - \delta_{COI}| \leq \delta_{MAX} \quad i = 1, 2, \dots, NG \quad (11)$$

$$\delta_{COI} = \frac{\sum_{i=1}^{NG} H_i \delta_i}{\sum_{i=1}^{NG} H_i} \quad i = 1, 2, \dots, NG \quad (11)$$

where (2) and (3) are active and reactive power balance equations; (4)–(8) are limits of active and reactive power output, voltage magnitude, transformer tap setting, and line loading respectively; (9) is swing equation that describes transient behavior of a synchronous generator; (10) is the transient stability limit; P_{Di} and Q_{Di} are the active and reactive power demands at bus i ; Q_{Gi} is the reactive power generation at bus i ; V_i and V_j are the voltage magnitudes at buses i and j ; G_{ij} and B_{ij} are the real and imaginary parts of the ij -th element of the admittance matrix (Y_{bus}); θ_{ij} is the difference of voltage angles between buses i and j ; T_i is the tap setting of the i -th transformer; S_{Li} is the line loading at line i ; N , NL , and NT are the numbers of buses, lines, and transformers; ω_R and ω_i are the rated rotor speed and rotor speed; P_{mi} and P_{ei} are the mechanical input and electrical output of the i -th generator; δ_i and δ_j are the rotor angles of the i - and j -th generators; H_i and D_i are the inertia constant and the damping coefficient and of the i -th generator; δ_{COI} is the position of the center of inertia (COI); δ_{MAX} is the maximum allowable deviation of the generator rotor angle with respect to COI. The subscripts x_{\max} and x_{\min} indicate the upper and lower limits of variable x .

C. Problem Formulation

According to subsections *A* and *B*, the TSCOPF problem has now been formulated as follows:

$$\begin{aligned} & \text{Minimize} \quad (1) \\ & \text{Subject to} \quad (2)–(11) \end{aligned} \quad (12)$$

D. Enforcement of TSCOPF constraints

For the equality constraints, the power balance equations shown in (2) and (3) are satisfied by Newton-Raphson based power flow calculation while the swing equations are met by the proposed neural network combined with time-domain simulation. The full details for handling the swing equations will be described in Section III.

For the inequality constraints, the penalty function is adopted to deal with all operating limits appeared in (4)–(8) and (10) so that the original constrained optimization problem is transformed to an unconstrained one as follows:

$$\begin{aligned} F_{ext} = & \sum_{i=1}^{NG} f_i(P_{Gi}) + K_p [h(P_{slack})] + K_q \sum_{i=1}^{NG} h(Q_{Gi}) \\ & + K_v \sum_{i=1}^{NLB} h(V_{Li}) + K_s \sum_{i=1}^{NL} h(S_{Li}) + K_R \end{aligned} \quad (13)$$

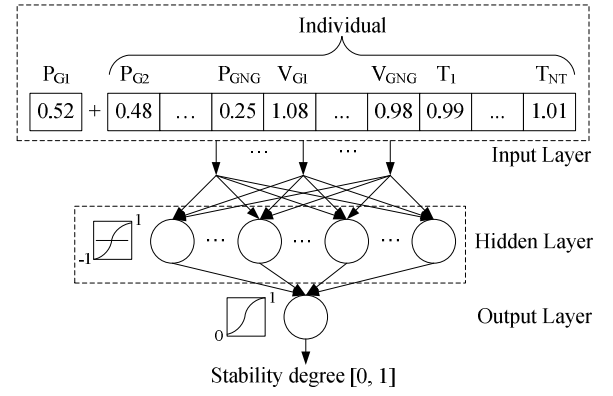


Fig. 1. Architecture of the proposed neural network.

where, K_p , K_q , K_v , and K_s are penalty weights of active power output of slack bus (P_{slack}), reactive power output of generator bus, load bus voltage magnitude, and line loading respectively; K_R is a penalty constant for transient stability limit; $h(P_{slack})$, $h(Q_{Gi})$, $h(V_{Li})$, and $h(S_{Li})$ are the penalty functions of the related variables. Note that the value of penalty function grows with a quadratic form when the constraints are violated and is 0 in the region where constraints are not violated.

The active power generation limits of all generator buses except for slack bus, voltage limits of all generator buses, and transformer tap setting limits are not included in (13), since these control variables are randomly created within their feasible limits during the proposed algorithm process. In conclusion, (13), already considering all inequality constraints, will be used as the new objective function to be minimized.

III. TRANSIENT STABILITY ASSESSMENT

This paper proposes the combination of time-domain simulation and neural network to evaluate the system transient stability. The neural network, which is less time-consuming, is first used to classify the individual into three regions, namely *stable*, *unstable*, and *critical* regions using pre-set thresholds and then time-domain simulation will be performed with only individual classified in the *critical* region. Instead of directly evaluating the system in terms of only the *stable* and *unstable* regions, the thresholds are introduced to account for the inherent error of the neural network.

Fig. 1 depicts the architecture of the proposed network. The proposed feed-forward network consists of inputs, one or more hidden layers, and one output layer. The inputs consist of the individual of AEP and P_{slack} . The hidden layers consist of neurons with the tan-sigmoid transfer function whereas the output layer consists of a single neuron with the log-sigmoid transfer function. A single output of the network signifies the stability degree of the individual. The stability degree is measured by the 0.05-gain sigmoid function $[(Sigmf(X))]$ of the difference between δ_{MAX} and maximum rotor angle deviation among all generators (δ_{MAXdiv}) as shown in Fig. 2. If δ_{MAXdiv} is lower than δ_{MAX} , the value of X will be a positive number, and vice versa. The individual that leads to very high degree of stability (high positive X) or instability (high negative X) will have the output near 1 or 0 respectively. When δ_{MAXdiv} is exactly equal

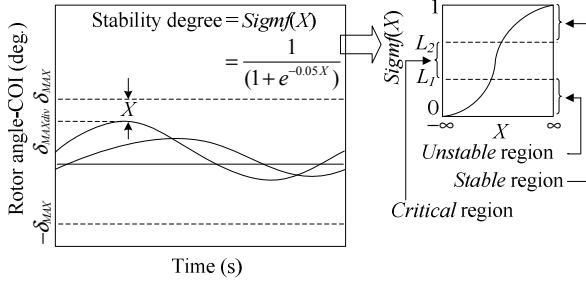


Fig. 2. Output of the proposed neural network.

P _{G2}	P _{GNG}	V _{G1}	V _{GNG}	T ₁	T _{NT}
0.48	...	0.25	1.08	...	0.98
				0.99	...
					1.01

Fig. 3. Real number coding solution (individual).

to δ_{MAX} , the output becomes 0.5. The criterion to perform time-domain simulation is determined by the output of the neural network. Namely, if the output is between the thresholds L_1 and L_2 (*critical region*), time-domain simulation is performed for the individual to scrutinize the transient behavior. Otherwise, the transient stability is immediately estimated without time-domain simulation i.e. output $< L_1$ means *unstable* and output $> L_2$ means *stable*.

IV. AEP FOR TSCOPF

Evolutionary programming (EP) [8] is one of the population-based heuristic algorithms, which searches for the optimal solution by evolving a set of candidate solutions, namely individuals, over a number of iterations through mutation and selection. An individual in a population represents a candidate solution coded by real number. For TSCOPF problem, each individual consists of control variables that include P_G of all generator buses excluding a slack bus, V_G of all generator buses, and T as shown in Fig. 3.

Generally, the main parameters of EP, i.e. population size (N_p), decaying mutation rate (a), and maximum generation (G_{max}) have to be predefined. Since the efficiency and run time of EP are strongly influenced by these parameters especially by N_p , their optimal setting is needed and normally obtained through the time-consuming trials and error.

In this paper, an adaptive evolutionary programming (AEP), which starts with a single-individual population and then changes the population size adaptively, is proposed. The population adaptation rule is based on the idea in [7]. The concept is that a population that has many *good* individuals can benefit from the removal of their weakest individual, since it already possesses many good candidate solutions. On the other hand, a population that has many *bad* individuals can benefit from the addition of a new individual to increase the possibility of improvement. Note that in the case of a single-individual population, the removal will be voided. An individual is said to be *good*, if it has the higher fitness than its parent, and vice versa. Let $N_{p,i}$ and G_i be the population size and the number of *good* individuals of the i -th generation respectively. The adaptation rule for adding or removing an individual is described as follows:

$$N_{p,i+1} = \begin{cases} N_{p,i} + 1 & \text{if } U[0, N_{p,i}] > G_i \\ N_{p,i} - 1 & \text{if } U[0, N_{p,i}] < G_i \end{cases} \quad (14)$$

where $N_{p,i+1}$ is the population size of the $(i+1)$ -th generation and $U[0, N_{p,i}]$ is a uniform distribution between 0 and $N_{p,i}$.

The adaptation rule will not take place at each generation, since the individuals should be allowed to search the solution for some time. In this paper, the population size will be modified after N_p generations. This means the more the population size is, the longer time between two adaptations will be.

The main components of AEP for TSCOPF are as follows:

A. Initialization

A single individual in an initial population is randomly initialized using a set of uniform distribution ranging over the feasible limits of each control variable. If the summation of the initialized P_G of all generators is less than the total active power demand, the initialization will be recalculated.

B. Power Flow Solution and Transient Stability Assessment

Power flow calculation by Newton-Raphson method is performed for every individual during iterations to come up with all variables in the system, i.e. P_{slack} , Q_G , V_L , and S_L . After this, if any variable violates its limits, the penalty term will be introduced in the objective function given in (13).

Next, the stability degree of each individual will be evaluated against the considered contingency by the proposed neural network with the predefined thresholds L_1 and L_2 . If the stability degree of the individual falls in the *stable* or *unstable* region, the stability status is immediately identified. On the other hand, if the stability degree falls in the *critical* region, time-domain simulation is performed. During integration process of time-domain simulation, if any generator rotor angle with respect to COI deviates beyond the stability limit appeared in (10), time-domain simulation is stopped before the maximum integration time leading to the computational time saving. In the case of *unstable* evaluated by either the neural network or time-domain simulation, since the stability limit is here considered as a severe constraint, the objective function is penalized by the large number K_R as appeared in (13).

C. Fitness Evaluation

After the power flow calculation and transient stability assessment, the fitness of each individual in a population will be evaluated according to (15).

$$ft_k = 1/F_{ext,k} \quad (15)$$

where ft_k and $F_{ext,k}$ are values of the fitness and the extended objective function of the k -th individual.

D. Mutation and Selection

An offspring individual is produced from a parent individual on a one-by-one basis. Each control variable of the k -th offspring is computed as follows:

$$c'_{k,i} = c_{k,i} + N(0, \sigma_{k,i}^2) \quad (16)$$

$$\sigma_{k,i} = (x_{k,i}^{max} - x_{k,i}^{min}) \left(\frac{(ft_{max} - ft_k)}{ft_{max}} + a^g \right) \quad (17)$$

where $c'_{k,i}$ and $c_{k,i}$ are the i -th control variable of the k -th offspring and parent individual respectively; $N(0, \sigma_{k,i}^2)$ is a Gaussian random number with a mean of zero and standard deviation of $\sigma_{k,i}$; and $x_{k,i}^{\max}$ are $x_{k,i}^{\min}$ the upper and lower limits of the i -th control variable of the k -th parent individual; ft_{\max} is the maximum fitness in the parent population; a is the decaying mutation rate, which is a positive constant number slightly less than one; g is the generation counter. If the value of any control variable mutated by (16) exceeds its corresponding limits, or the summation of the mutated P_G of all generators is less than the total active power demand, the mutation process will be recalculated.

After creating the offspring, the parent and offspring populations are combined together forming a combined population. Tournament scheme is used to perform the selection. By comparing the fitness with other opponent individuals, scoring for each individual in the combined population can be obtained. Lastly, the individuals with the higher score will be chosen to form the new parent population for the next iteration.

E. AEP Procedure for TSCOPF

The procedure of AEP algorithm for TSCOPF problem is described as follows:

- Step 1: Load system data, AEP parameters, a trained neural network, set $g = 1$ and $R = 1$.
- Step 2: Create a single individual of the initial population.
- Step 3: Perform power flow calculation and stability assessment. Calculate the fitness for an initial individual and set best solution (S_b) = the initial individual.
- Step 4: Create the offspring population through the mutation.
- Step 5: Perform power flow calculation and stability assessment. Calculate the fitness for offspring. If ft of the fittest individual in the offspring population $>$ that of S_b , set (S_b) = that individual.
- Step 6: Select the new parent population for the next iteration by the tournament scheme.
- Step 7: If $R = N_p$, modify the population size by (14) and set $R = 0$. Otherwise, the population size is the same.
- Step 8: If $g < G_{\max}$, set $g = g + 1$, $R = R + 1$, and go back to Step 4. If not, terminate the process and S_b is the TSCOPF solution.

Please note that R is the number of iterations since the last population's adaptation.

V. SIMULATION RESULTS AND DISCUSSION

The IEEE 30-bus system is used as the test system. The single-line diagram of the system is depicted in Fig. 4. The bus and line data of the system can be found in [9]. The transformer operating range is set between 0.9 and 1.1. A single contingency (A) shown in Fig. 4 is considered in the TSCOPF problem. The contingency is a three-phase grounding fault at $t = 0$ s and cleared by removing the line 2-5 at $t = 0.35$ s. In time-domain simulation, the integration time step is 0.01 s, the maximum integration time is 1.5 s, and δ_{MAX} is 120 degrees.

To demonstrate the effectiveness of the proposed method, two different types of generator fuel cost curve, i.e. quadratic

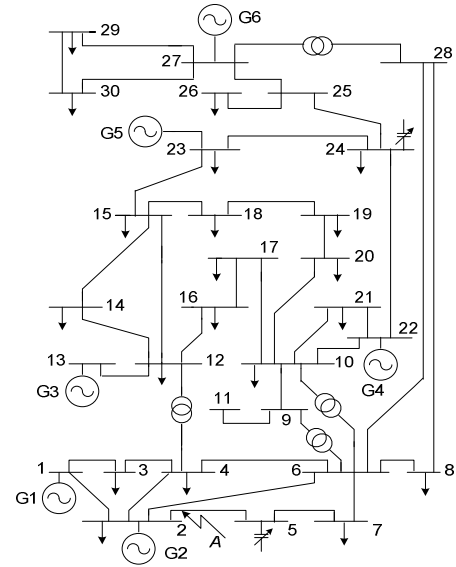


Fig. 4. Single-line diagram of IEEE 30-bus system.

cost curve (f_q) and quadratic cost curve superimposed by sine component (f_s), are considered. Those cost curves are mathematically expressed as follows:

$$f_q(P_G) = a + bP_G + cP_G^2 \quad (18)$$

$$f_s(P_G) = a + bP_G + cP_G^2 + |d \sin(e(P_{G,\min} - P_G))| \quad (19)$$

All simulations are developed on MATLAB and implemented on a personal computer with Intel Pentium IV 3.8 GHz processor and 512 MB memory.

A. Study of the Proposed Neural Network

As known, even though the number of neurons in the hidden layer should be large enough to model the complex function, the too large number of neurons can cause overfitting leading to degradation of network generalization. To avoid the overfitting problem, the early stopping is adopted in training process. For the test system, there are 16 input neurons (15 variables from individual and 1 variable from P_{slack}) and 1 output neuron ($[(\text{Sigmf}(X))]$). Modified from Newton's method, the fast Levenberg-Marquardt algorithm is chosen to train the proposed network with 3000 training and 1000 validation patterns. In each training or validation pattern, the inputs are randomly generated within their feasible operating range. The maximum growth factor is set to 2. The performance of the trained network is measured by the mean sum squares of the network errors ($MSEs$) as follows:

$$MSE = 1/N_s \sum_{i=1}^{N_s} (r_i - m_i)^2 \quad (20)$$

where r_i is the i -th actual output from time-domain simulation; m_i is the i -th output value from the neural network; N_s is the number of patterns (training or validation patterns).

Table I shows the $MSE \times 10^{-3}$ of the 5 different network architectures trained with 3000 training and 1000 validation patterns when the contingency A is considered. Moreover, the $MSE \times 10^{-3}$ of the independent 1000 testing patterns, which

TABLE I
MSE AND THE NUMBER OF MIS OF DIFFERENT ARCHITECTURES

Architecture	$MSE \times 10^{-3}$			The number of MIS	
	Training	Validation	Testing	Without thresholds	With thresholds
16/20/5/1	0.303	1.440	1.619	61	9
16/25/5/1	0.445	1.607	1.555	68	15
16/30/5/1	0.095	1.470	1.550	31	6
16/35/5/1	0.568	1.834	1.664	73	25
16/40/5/1	0.435	1.448	1.619	57	19

are not used during training process, is provided to compare the performance of different architectures. Besides, out of 5000 patterns (training + validation + testing), the number of misclassified individuals (MIs), i.e. the individual actually leads to *stable* case but the neural network classifies it into the *unstable* region, and vice versa, is given for both with and without threshold cases. The thresholds L_1 and L_2 are set to 0.45 and 0.55. The architecture 16/20/5/1 means that there are 16 input neurons, 20 neurons in the first hidden layer, 5 neurons in the second hidden layer, and one neuron of the output.

From the table, the architecture 16/30/5/1, which offers the smallest *MSE* for both training and testing sets and the smallest number of MIS, is chosen to estimate the transient stability. Note that the 6 misclassified individuals of the selected architecture with thresholds are 0 from training set, 4 from validation set and 2 from testing set. This number represents 0.12% of overall misclassification. All 6 misclassifications are safe for system operator, since all of them are the case that the system is *stable* but the neural network classifies it into the *unstable* region. It is very harmful if the system is *unstable* but the neural network classifies it into the *stable* region.

B. TSCOPF Results by AEP

Numerical examples are divided into 2 cases as follows:

Case 1: All generators' cost curves are represented by (18).

The cost coefficients can be found in [9].

Case 2: The cost curves of the 2-nd and 3-rd generators are replaced by (19). The cost coefficients of the 2-nd generator i.e. a_2, b_2, c_2, d_2 , and e_2 , are 0, 2.5, 0.01, 35, and 0.118 respectively. The coefficients of the 3-rd generator i.e. a_3, b_3, c_3, d_3 , and e_3 are 0, 3.7, 0.022, 21, and 0.236 respectively.

For the AEP parameter setting, the decaying mutation rate (a) is 0.97 and G_{\max} is 200. Note that the parameter a should be set according to the G_{\max} to prevent premature convergence. All penalty weights shown in (13) are set to 1000.

First, Table II shows the OPF results of 20 independent runs solved by AEP. To show the effectiveness of AEP, the OPF results solved by the conventional EP with $N_p = 8$ are also given. The results show AEP can obtain the cheaper fuel cost and requires the shorter computational time than EP in both cases. The reason why AEP spends less run time than EP is because the average population size of AEP is smaller than that of EP. In addition, in Case 1, the AEP solution is even better than that of PSO (576.63 \$/hr), GA (576.64 \$/hr) and

TABLE II
COMPARISON OF OPF RESULTS SOLVED BY AEP AND EP

Result	Case 1		Case 2	
	AEP	EP	AEP	EP
Avg. cost (\$/hr)	575.00	575.05	605.94	605.63
Worst cost (\$/hr)	575.28	575.45	607.58	608.63
Best cost (\$/hr)	574.41	574.52	603.92	604.33
Standard deviation	0.22	0.23	0.93	1.13
Avg. population size	5.43	8	6.10	8
Avg. run time (s)	31.11	41.12	35.10	43.84

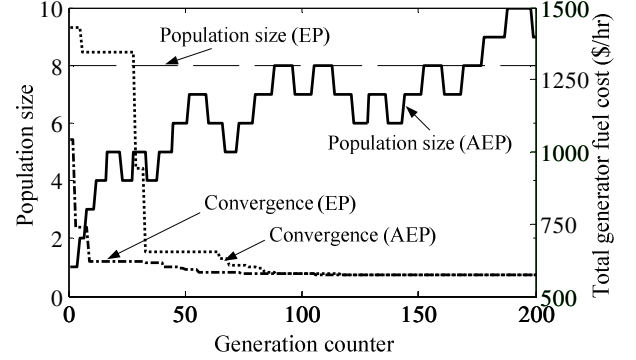


Fig. 5. Population size and convergence of EP and AEP in Case 1 (OPF).

TABLE III
TSCOPF RESULTS BY AEP WITH AND WITHOUT THE NEURAL NETWORK

	Case 1		Case 2		
	With neural network	Yes	No	Yes	No
Avg. cost (\$/hr)		585.00	585.15	625.54	625.76
Worst cost (\$/hr)		585.91	585.95	627.71	628.40
Best cost (\$/hr)		584.16	584.19	624.21	624.18
Avg. population size		6.48	5.98	6.99	6.69
% U_{TDS}		38.65	100	3.28	100
Avg. run time (s)		235.88	577.73	79.50	711.29
% Time reduction		59.17	-	88.82	-

sequential quadratic programming (576.89 \$/hr) all of which are reported in [4]. Based on the AEP and EP best solutions in Case 1, the population size and convergence are plotted in Fig. 5. From the figure, AEP converges to the solution slower than EP, since the population size of AEP is less than that of EP during the first 100 generations.

Next, for Cases 1 and 2, the TSCOPF solutions of 20 independent runs solved by AEP with and without the neural network are tabulated in Table III. The percentage of utilization of time-domain simulation (U_{TDS}) for transient stability assessment is also given. The more frequent the time-domain simulation is run, the longer the computational time will be. With the help of the neural network, the computational time is decreased around 60 % in Case 1 and up to 89 % in Case 2 without degrading the quality of the solution. This confirms that AEP with the neural network can greatly lessen the computational burden regarding the transient stability constraints without loss of the ability to locate the optimal solution.

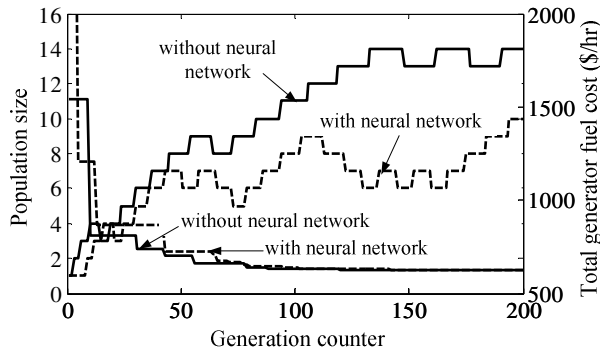


Fig. 6. Population size and convergence of AEP in Case 2 (TSCOPF).

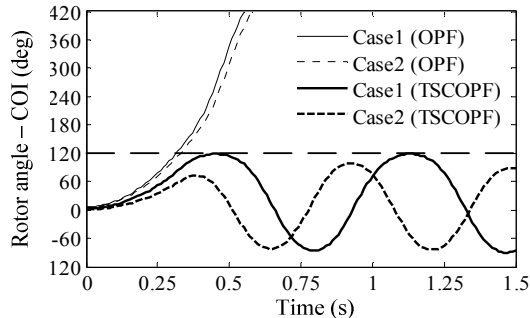


Fig. 7. Rotor angle curves based on the best AEP-based OPF and TSCOPF solutions in Cases 1 and 2 after the contingency *A*.

By comparing OPF and TSCOPF results from Tables II and III at the same case, the fuel costs of TSCOPF are more costly than those of OPF. This is because the additional transient stability constraints are imposed in the OPF.

Based on the best TSCOPF solutions in Case 2, the population size and convergence of AEP with and without the neural network are plotted in Fig. 6. From the figure, the convergence speed of both cases is comparatively the same.

After the contingency *A*, the rotor angles with respect to COI of the 2-nd generator (the largest swing) in Cases 1 and 2 based on the best OPF and TSCOPF solutions solved by AEP are plotted in Fig. 7. Obviously, TSCOPF can guarantee the system stability after the considered contingency whereas OPF cannot. The operating points of the best AEP-based OPF and TSCOPF solutions in Cases 1 and 2 are given in Table IV.

VI. CONCLUSIONS

This paper proposes an AEP method with a neural network for solving TSCOPF problem in which the population size is adjusted adaptively. First, the OPF results show that AEP is superior to the conventional EP in both finding the optimal solution and saving the computational time. Next, AEP with the selected neural network is proved to be a promising method for TSCOPF problem. The future work will investigate the applicability of the propose method for a multi-contingency TSCOPF problem.

VII. REFERENCES

[1] J. A. Momoh, *Electric Power System Applications of Optimization*, New York: Marcel Dekker, 2001.

TABLE IV
OPF AND TSCOPF RESULTS BY AEP IN CASES 1 AND 2

Result	Case 1		Case 2	
	OPF	TSCOPF	OPF	TSCOPF
P_{G1} (MW)	43.96	52.21	44.37	55.52
P_{G2} (MW)	57.92	39.00	53.25	26.65
P_{G3} (MW)	17.39	19.77	13.29	13.31
P_{G4} (MW)	22.95	24.17	22.84	28.57
P_{G5} (MW)	16.99	17.44	18.60	20.89
P_{G6} (MW)	32.38	39.32	39.47	47.05
V_{G1} (p.u.)	1.05	0.98	1.04	1.01
V_{G2} (p.u.)	1.04	0.98	1.04	1.01
V_{G3} (p.u.)	1.09	1.06	1.07	1.05
V_{G4} (p.u.)	1.04	1.01	1.01	1.00
V_{G5} (p.u.)	1.05	1.02	1.03	1.01
V_{G6} (p.u.)	1.06	1.04	1.05	1.04
T_1 (bus 6-9)	0.97	0.97	1.04	0.95
T_2 (bus 6-10)	0.99	0.99	1.00	1.00
T_3 (bus 4-12)	1.02	0.97	1.03	1.06
T_4 (bus 28-27)	1.08	1.06	1.09	1.05
Fuel cost (\$/hr)	574.41	584.16	603.92	624.21

- [2] D. Gan, R. J. Thomas, and R. D. Zimmerman, "Stability-Constrained Optimal Power Flow," *IEEE Trans. Power Systems*, vol. 15, no. 2, pp. 535–540, May 2000.
- [3] Y. Yuan, J. Kubokawa, and H. Sasaki, "A Solution of Optimal Power Flow with Multicontingency Transient Stability Constraints," *IEEE Trans. Power Systems*, vol. 18, no. 3, pp. 1094–1102, Aug. 2003.
- [4] N. Mo, Z. Y. Zou, K. W. Chan, and T. Y. G. Pong, "Transient stability constrained optimal power flow using particle swarm optimization," *IET Generation Transmission and Distribution*, vol. 1, no. 3, pp. 476–483, May 2007.
- [5] K. Y. Chan, S. H. Ling, K. W. Chan, H. H. C. Lu, and G. T. Y. Pong, "Solving Multi-Contingency Transient Stability Constrained Optimal Power Flow Problems with an Improved GA," in *Proc. 2007 IEEE Congress on Evolutionary Computation*, pp. 2901–2908.
- [6] H. R. Cai, C. Y. Chung, and K. P. Wong, "Application of Differential Evolution Algorithm for Transient Stability Constrained Optimal Power Flow," *IEEE Trans. Power Systems*, vol. 23, no. 2, pp. 719–728, May 2008.
- [7] Y. Cooren, M. Clerc, and P. Siarry, "Initialization and Displacement of the Particles in TRIBES, a Parameter-Free Particle Swarm Optimization Algorithm," *Adaptive and Multilevel Metaheuristics*, Springer Berlin / Heidelberg, pp. 199–219, 2008.
- [8] J. Yuryevich and K. P. Wong, "Evolutionary Programming Based Optimal Power Flow Algorithm," *IEEE Trans. Power Systems*, vol. 14, no. 4, pp. 1245–1250, Nov. 1999.
- [9] R. Zimmerman, E. Murillo-Sánchez, and D. Gan, "MATPOWER: a MATLAB Power System Simulation Package," 2006.

VIII. BIOGRAPHIES

Kritsana Tangpatiphan (S'08) received the B.Eng. in Electrical Engineering, Thammasat University, Thailand, in 2002 and M.Eng. in electric power system management from Asian Institute of Technology (AIT), Thailand, in 2004. Currently, he is pursuing the Ph.D. degree at the University of Tokyo, Japan, with MEXT scholarship. His interests include the application of artificial intelligence techniques to power system optimization problems. He is a student member of IEEJ and IEEE.

Akihiko Yokoyama (M'78) was born in Osaka, Japan, on October 9, 1956. He received B.S., M.S. and Dr. Eng from the University of Tokyo, Tokyo, Japan in 1979, 1981 and 1984, respectively. He has been with Department of Electrical Engineering, the University of Tokyo since 1984 and currently a professor in charge of Power System Engineering. He is a member of IEEJ, IEEE and CIGRE.